X International Conference on Computational Methods for Coupled Problems in Science and Engineering
COUPLED PROBLEMS 2023
M. Papadrakakis, B. Schrefler and E. Oñate (Eds)

ON THE CHOICE OF TIME WINDOW LENGTH FOR WAVEFORM ITERATIONS FOR COUPLED PROBLEMS

NIKLAS KOTARSKY*, AND PHILIPP BIRKEN†

*Center for Mathematical Sciences
Lund University
Box 118, 22100 Lund, Sweden
e-mail: niklas.kotarsky@math.lu.se

†Center for Mathematical Sciences
Lund University
Box 118, 22100 Lund, Sweden
e-mail: philipp.birken@math.lu.se, web page: https://www.maths.lu.se/staff/philipp-birken/

Key words: Coupled Problems, Waveform iterations, Time windows, Heat transfer

Abstract. We consider waveform iterations for dynamic coupled problems with respect to the role of time window length. We review existing theoretical results about the error of waveform iterations and the role of the time window length. Furthermore, we present numerical results for waveform iterations with both time adaptive sub solvers and with fixed time steps. This way, we are able to give a recommendation on the choice of the time window. The use of time windows can lead to an increase in efficiency. For fixed time grids, we can reliably achieve a small performance increase. For time adaptive solvers, more research is needed.

1 Introduction

We are interested in coupled partial differential equations defined on two domains that interact with each other on a lower dimensional interface. Examples are steel quenching where hot steel is cooled down by blowing cold air over it, or a feather moving in the wind. Here we use a partitioned algorithm where two different solvers are used for the sub problems. Furthermore, the two sub problems are not necessarily on the same time scale, thus one wants to allow for different timestep sizes in the two solvers. Also, using a constant timestep for transient problems is not efficient. Thus, one wants to use a time adaptive solver, which automatically chooses the timestep based on a local error estimate instead.

This can be achieved by so called waveform iterations. They where originally developed to solve systems of coupled ODEs coming from electrical circuits in the 1970s ([10, 11]) to allow for parallelization. They have also been successfully applied to coupled PDEs, for example in [13, 5, 9], where applications in heat transfer and fluid structure interaction were studied.

Convergence of waveform iterations has mostly been studied for the ODE case in various continuous and discrete settings see, [10, 11]. For ODEs, waveform iterations achieve superlinear convergence. In [1], convergence of the waveform iteration is proven for time adaptive sub solvers under the assumption of the time grid's convergence.

The convergence theory for PDEs is not as exhaustive as for ODEs. Convergence conditions for linear PDEs were derived in [2] and [3] for both the semi discrete case as well as the fully discrete case. One of the big challenges for many coupled PDEs, such as coupled heat equations, is that waveform iterations do not converge for all material parameters. To obtain fast convergence one has to use some kind of acceleration like under relaxation. This is done in [9] and [5] for the fully discrete case. In [12], super linear convergence is proven for the fully continuous linear heat equation in 1D with all material parameters equal to 1.

In both the ODE and PDE case, the error increases with the simulation time T_f, which may cause instabilities as well as slow convergence. To avoid these instabilities, it is common practice to split the whole time interval into multiple shorter time windows, onto which the waveform iterations are successively applied. Whilst the time window length affects the convergence speed, it is not clear how large or short the time windows should be to maximize efficiency. The other aspect is that for every time window, we make a coupling error that is controlled by the tolerance in the termination criterion. It is thus possible that the accumulation of this coupling error affects the time integration error, forcing one to reduce the tolerance, effectively negating all positive benefits of using shorter time windows. In [14], it is shown that shorter time windows can increase the energy efficiency for the ODE case. For PDEs, there has been little research on how to choose the size of the time window.

In this article, we review existing theoretical results about the error of waveform iterations and the role of the time window length. Furthermore, we present numerical results for waveform iterations with both time adaptive sub solvers and with fixed time steps. This way, we are able to give a recommendation on the choice of the time window for fixed time grids. For our test, case the experiments show that shorter time windows require fewer waveform iterations, yielding an increase in performance for the fixed time step case. A small increase in performance can also be observed for the adaptive time case. However, one would have to use non equidistant time windows to achieve this increase in performance reliably, which is beyond the scope of this article.

2 Waveform iterations

Consider the following ODE on the interval $[0, T_f]$:

$$\dot{w} = g(w, v), \quad w(0) = w_0, \tag{1}$$
$$\dot{v} = h(v, w), \quad v(0) = v_0. \tag{2}$$

To define our waveform iteration, we divide the interval $[0, T_f]$ into a finite number of time windows $[T_{w-1}, T_w]$. In the following, without loss of generalization, we assume that there is only one time window $[0, T_f]$. The continuous Gauß-Seidel or serial waveform iteration is then given by

$$\dot{w}^{k+1} = g(w^{k+1}, v^k), \quad w^{k+1}(0) = w_0, \tag{3}$$
$$\dot{v}^{k+1} = h(v^{k+1}, w^k), \quad v^{k+1}(0) = v_0, \tag{4}$$

where the starting guess $v^0(t) = v_0$ is commonly used. In this paper we use the termination criterion

$$||v^{k+1}(T_w) - v^k(T_w)||/||v_0|| \leq Tol_{WR}, \tag{5}$$

where T_w denotes the end of the time window and $\|\cdot\|$ is a vector norm.

A discrete waveform iteration is given by discretizing both sub problems in time on the time grids $\{t_w^{i,k}\}_{i=0}^{N_w^k}$ and $\{t_v^{i,k}\}_{i=0}^{N_v^k}$ respectively. The two time grids are not assumed to be matching. Thus, one has to use interpolation $I(w^k, \{t_w^{i,k}\}_{i=0}^{N_w^k})$ in the discrete waveform iteration, yielding

$$\dot{w}^{k+1,n+1} = g(w^{k+1}, I(v^k, \{t_v^{i,k}\}_{i=0}^{N_v^k}), \quad w^{k+1}(0) = w_0, \tag{6}$$

$$\dot{v}^{k+1,n+1} = h(v^{k+1}, I(w^k, \{t_w^{i,k}\}_{i=0}^{N_w^k})), \quad v^{k+1})(0) = v_0. \tag{7}$$

The sub problems are then discretized using any time integration method.

The simplest way to speed up the convergence is to use under relaxation where the next WR iterate is given as a weighted average of the previous iterates, yielding

$$\dot{w}^{k+1,n+1} = g(w^{k+1}, I(v^k, \{t_v^{i,k}\}_{i=0}^{N_v^k}), w^{k+1}(0) = w_0, \tag{8}$$

$$\dot{\hat{v}}^{k+1,n+1} = h(\hat{v}^{k+1}, I(w^k, \{t_w^{i,k}\}_{i=0}^{N_w^k})), \hat{v}^{k+1} = v_0, \tag{9}$$

$$v^{k+1} = \theta\hat{v}^{k+1} + (1-\theta)v^k, \tag{10}$$

with the relaxation parameter $\theta \in [0, 1]$. The optimal relaxation parameter θ is problem and discretization dependent.

2.1 Convergence results for waveform iterations

Convergence of waveform iterations has mostly been studied for the ODE case in various continuous and discrete settings, see for example [10, 11]. For ODEs, waveform iterations achieve superlinear convergence with an error bound of the form

$$||e^k||_{[0,T_f]} \leq \frac{(CT_f)^k}{k!}||e^0||_{[0,T_f]},$$

where $C > 0$ is a constant depending on the Lipschitz-constant of the coupled ODEs as well as their time discretization. The norm $||.||_{[0,T_f]}$ is defined as $||e^k||_{[0,T_f]} := \sup_{t\in[0,T_f]} ||e^k(t)||$. In [1], convergence of the waveform iteration is proven for time adaptive sub solvers under the assumption of the time grid's convergence.

The convergence theory for PDEs is not as exhaustive as for ODEs. One of the big challenges for many coupled PDEs, such as coupled heat equations, is that waveform iterations do not converge for all material parameters. To obtain fast convergence one has to use some kind of acceleration like under relaxation. This is done in [8, 9, 5] for the fully discrete case. In [12], two coupled 1D heat equation with all material parameters equal to one are analyzed in the fully continuous setting and super linear convergence is proven for the relaxation parameter $\theta = 1/2$. Furthermore, it is shown that the waveform iteration converges to the exact solution in two iterations if the domains are of the same size.

The semi discrete and discrete case for linear PDEs was analysed in [2] and [3]. The PDEs are discretized in space by linear finite elements to yield an IVP of the form

$$A\dot{u} + Bu = f(t). \tag{11}$$

Then, a general splitting of the form

$$M_A\dot{u}^{k+1} + M_B u^{k+1} = N_A u^k + N_B u^k f(t), \tag{12}$$

where $M_A + N_A = A$ and $M_B + N_B = B$ is studied. The main idea is to analyse the waveform operator by splitting it into one linear part $K = M_B^{-1} N_B$ and one nilpotent part

$$K_c = e^{-M_B^{-1} M_A t} M_B^{-1} (N_A - M_A M_B^{-1} N_B), \tag{13}$$

yielding

$$u^{k+1} = K u^k + \int_0^t K_c(t-s) u(s) ds + F(t). \tag{14}$$

The error estimate is then given by

$$||e^k||_{[0,T_f]} \leq \left(\sum_{j=0}^{k} \binom{k}{j} ||K||^{k-j} ||K_c||^j_{[0,T_f]} \frac{T_f^j}{j!} \right) ||e^0||_{[0,T_f]}. \tag{15}$$

The asymptotic convergence behavior is only determined by K and in [2] it is shown that this iteration converges linearly if the spectral radius fulfills $\rho(K) = \rho(K) < 1$ and super linearly if $\rho(K) = 0$. However, due to the nilpotent operator, the iteration does not necessarily converge monotonously and the error could even increase in the first few iterations. It is difficult to get a better understanding of the convergence behavior, since this involves the pseudo spectra for the operators K and K_c. The fully discrete case where the IVP (11) is discretized by a multi step method is analysed in [3]. There it is shown that the waveform iterations converge if the one step method converges.

These results show that the length of the time window effects the convergence of the waveform iteration. However, there are to our knowledge no further results detailing the convergence of waveform relaxation for the fully discrete case. Thus, we investigate the effect of time window length numerically.

3 Model problem and discretization

As a model problem we use two coupled linear heat equations, given as follows:

$$\alpha_1 \dot{u}_1(t,x) - \lambda_1 \Delta u_1(t,x) = 0, \quad x \in \Omega_1, \tag{16}$$
$$u_1(x,t) = 0, \quad x \in \partial\Omega_1 \setminus \Gamma, \tag{17}$$
$$u_1(x,t) = u_2(x,t), \quad x \in \Gamma, \tag{18}$$
$$u_1(x,0) = u_{0_1}(x), \quad x \in \Omega_1, \tag{19}$$

$$\alpha_2 \dot{u}_2(t,x) - \lambda_2 \Delta u_2(t,x) = 0, \quad x \in \Omega_2, \tag{20}$$
$$u_2(x,t) = 0, \quad x \in \partial\Omega_2 \setminus \Gamma, \tag{21}$$
$$\lambda_2 \frac{\partial u_2(x,t)}{\partial n} = \lambda_1 \frac{\partial u_1(x,t)}{\partial n}, \quad x \in \Gamma, \tag{22}$$
$$u_2(x,0) = u_{0_2}(x), \quad x \in \Omega_2, \tag{23}$$

where $t \in [0, T_f]$, $\Omega_1 = [-1, 0] \times [0, 1]$, $\Omega_2 = [0, 1] \times [0, 1]$ and $\Gamma = \Omega_1 \cap \Omega_2$. The constants λ_1 and λ_2 denote the thermal conductivities for the materials Ω_1 and Ω_2. Likewise, α_m for $m = 1, 2$

Material	α $[J/(Km^3)]$	λ $[W/(mK)]$
Steel	3 471 348	49
Water	4 190 842	0.58
Air	1 299 465	0.024

Table 1: The different material parameters.

are constants defined by $\alpha_m = c_m \rho_m$, where ρ_m is the density and c_m the specific heat capacity of the material. The different material parameters used in the study are shown in Table 1. The initial value is given by $u(x,t) = 500 \sin(\pi y) \sin(\pi(x+1)/2)$.

This coupled problem will be solved iteratively using Dirichlet-Neumann waveform relaxations, see e.g. [6]. Here, we use the so called Gauß-Seidel variant, which solves the problems in sequence. First, the continuous Dirichlet problem on the time window $[0, T_f]$ is given by

$$\alpha_1 \dot{u}_1^{k+1}(t,x) - \lambda_1 \Delta u_1^{k+1}(t,x) = 0, \quad x \in \Omega_1, \tag{24}$$
$$u_1^{k+1}(x,t) = 0, \quad x \in \partial\Omega_1 \setminus \Gamma, \tag{25}$$
$$u_1^{k+1}(x,t) = u_\Gamma^k, \quad x \in \Gamma, \tag{26}$$
$$u_1^{k+1}(x,0) = u_{0_1}(x), \quad x \in \Omega_1, \tag{27}$$

where u_Γ^k denotes the interface temperature. Second, the Neumann problem on $[0, T_f]$ is given similarly by

$$\alpha_2 \dot{u}_2^{k+1}(t,x) - \lambda_2 \Delta u_2^{k+1}(t,x) = 0, \quad x \in \Omega_2 \tag{28}$$
$$u_2^{k+1}(x,t) = 0, \quad x \in \partial\Omega_2 \setminus \Gamma \tag{29}$$
$$\lambda_2 \frac{\partial u_2^{k+1}(x,t)}{\partial n} = q^{k+1}, \quad x \in \Gamma, \tag{30}$$
$$u_2^{k+1}(x,0) = u_{0_2}(x), \quad x \in \Omega_2, \tag{31}$$

where $q^{k+1} = \lambda_1 \frac{\partial u_1^{k+1}(x,t)}{\partial n}$ denotes the heat flux from the Dirichlet domain. Lastly, the relaxation step is given as

$$u_\Gamma^{k+1} = (1-\theta) u_\Gamma^k + \theta u_2^{k+1}|_\Gamma. \tag{32}$$

Both differential equations are discretized in space by a linear finite element method, yielding the IVP for the Neumann problem as: Find $u_{h_2} \in V$, s. t.

$$\int_{\Omega_2} \alpha_2(\dot{u}_{h_2}, v) + \lambda_2(\nabla u_{h_2}, \nabla v) dx + \int_\Gamma (q_h, v) dS = 0, \quad \forall v \in V, \tag{33}$$

where v is a test function, V is our finite element space, and q_h the discrete heat flux from the Dirichlet problem. The weak form of the Dirichlet problem is given similarly to the Neumann problem where the heat flux q_h has been replaced by a Dirichlet boundary condition. The

resulting IVPs for both sub problems are discretized with SDIRK2, as in [8] and [6]. For a general initial value problem $\dot{u} = f(u)$, the SDIRK2 method is given by

$$U_1 = u^n + a\Delta t f(t_n + a\Delta t, U_1) \tag{34}$$
$$u^{n+1} = u^n + (1-a)\Delta t_n f(t + a\Delta t, U_1) + a\Delta t f(u^{n+1}), \tag{35}$$

where $a = 1 - \sqrt{2}/2$.

To get to our discrete waveform iterations, the interface variables $u_{h_\Gamma}^{k+1}$ and q_h^{k+1} are interpolated using piecewise linear interpolation as in [6] and [7]. The heat flux from the Dirichlet problem is calculated using

$$\int_\Gamma (q_h^{k+1,n+1}, v) dS = \int_{\Omega_1} \alpha_1 \left(\frac{u_{h_1}^{k+1,n+1} - U_{1_{h_1}}}{a\Delta t}, v \right) + \lambda_1 (\nabla u_{h_1}, \nabla v) dx, \tag{36}$$

and the initial flux is calculated using

$$q_h(0) = \int_\Gamma \nabla u_1(x, 0) \cdot n ds. \tag{37}$$

The norm $||\cdot||$ for the convergence criterion (5) is in our case defined as $\sqrt{\sum_i \Delta x v_i^2}$, where Δx is the spatial mesh width. To improve the convergence speed of the waveform iteration, we use relaxation. Results for the optimal relaxation parameter in various continuous and discrete settings for the heat equation can be found in [12], [9], [4] and [5]. We use the relaxation parameter detailed in [6], which builds upon [8] for our test case, since it achieves a fast convergence rate for the linear heat equation in 2D.

A local error estimate for the SDIRK2 method is given by

$$l_{n+1} = (a - \hat{a})\Delta t_n f(t + a\Delta t, U_1) + (a - \hat{a})\Delta t f(U_2), \tag{38}$$

with $\hat{a} = 2 - \frac{5}{4}\sqrt{2}$. The timestep for the time adaptive solvers will then be given by a simple dead beat controller defined as $\Delta t^{n+1} = \Delta t^n (\frac{Tol_{TA}}{||l_{n+1}||_2})^{1/2}$ together with a initial timestep of $\Delta t = \frac{|T_f| Tol_{TA}^{1/2}}{100(1+||f(u_0)||_2)}$. The tolerance for time adaptivity is chosen as $Tol_{TA} = Tol_{WR}/5$ as done in [6] and [9].

4 Numerical Results

We now investigate the effect of the time window length numerically. The test case was implemented in Python by Peter Meisrimel and Azahar Monge with small modifications to allow for multiple time windows and can be found here: [15]. The spatial mesh width Δx was set to 1/100. To solve the arising linear systems, a direct solver is used, implemented in Scipy's sparse linear algebra library.

4.1 Constant time grids

We first consider fixed time grids and compare error and number of waveform iterations for different time steps and tolerances. The time grids were selected as in [6] such that both sub problems have similar CFL numbers. This is achieved by setting the step size ratio to

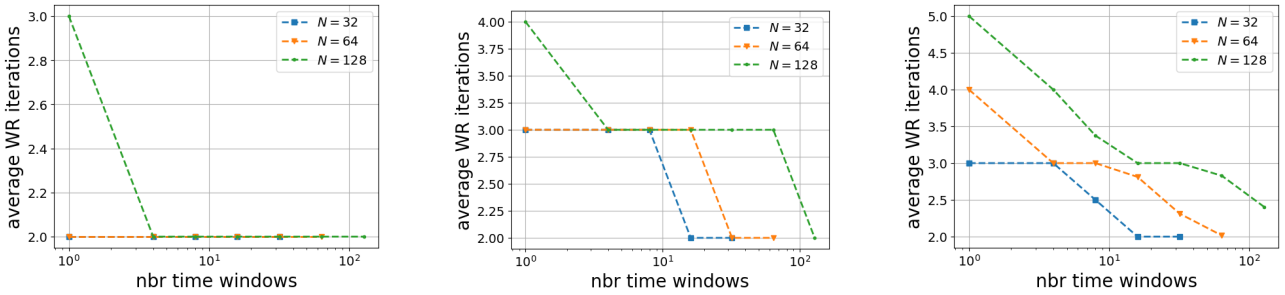

(a) Air-steel (b) Air-water (c) Water-steel

Figure 1: The average number of waveform iterations per time window over the number of time windows for the fixed time grid case.

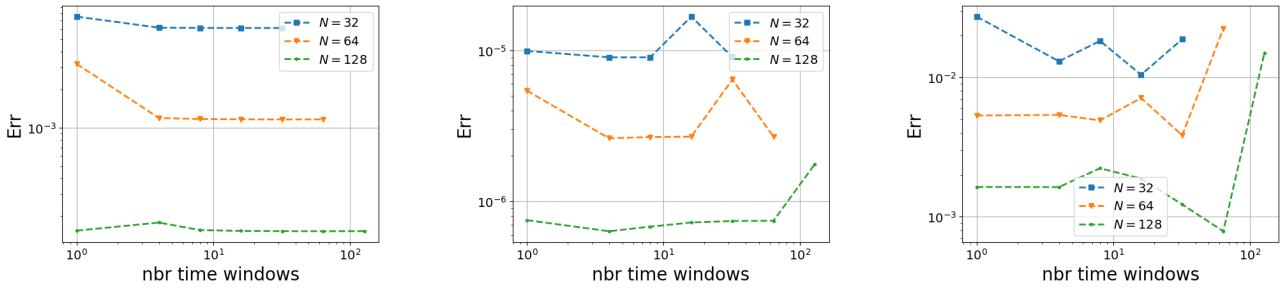

(a) Air-steel (b) Air-water (c) Water-steel

Figure 2: The time integration error over the number of time windows for the fixed time grid case described above.

$c_1 = \max(1, \lfloor D_2/D_1 \rfloor)$ and $c_2 = \max(1, \lfloor D_1/D_2 \rfloor)$, where $D_i = \lambda_i/\alpha_i$ for $i = 1, 2$. The stepsize for the sub solvers is then given by $\Delta t_i = T_f/(c_i N)$, where N denotes the number of base time steps. We choose $N = 32$, 64 and 128 and the simulation time T_f was set to 10^4 seconds. Instead of choosing the tolerance for the waveform iteration by trial and error, we computed the time integration error and chose the tolerance to be the error divided by 10, since one normally would want that the two error sources are comparable in magnitude. The error was measured by using a reference solution that was calculated with $N = 256$ together with a waveform tolerance of 10^{-8}. We now divide the interval $[0, T_f]$ into up to N_w equally sized time windows, where N_w divides N, since both solvers need to take an integer number of time step in each time window. For the same reason N_w is assumed to be less than N. We then measure the average number of iterations per time window as well as the time integration error for different number of time windows as shown in Figures 1 and 2.

The number of time windows affects the error, since every time window has a coupling error that is controlled by the tolerance Tol_{WR}. Thus, if the coupling error dominates the time integration error, then the accumulation of coupling error could cause an increasing error with the number of time windows. However, as can be seen in Figure 2, this was not the case in our testing, except for very large tolerances or coarse spatial grids (not shown). There is however some variation in the error in Figure 2. This can largely be explained by the fact that the termination criterion only considers the last time step of the time window.

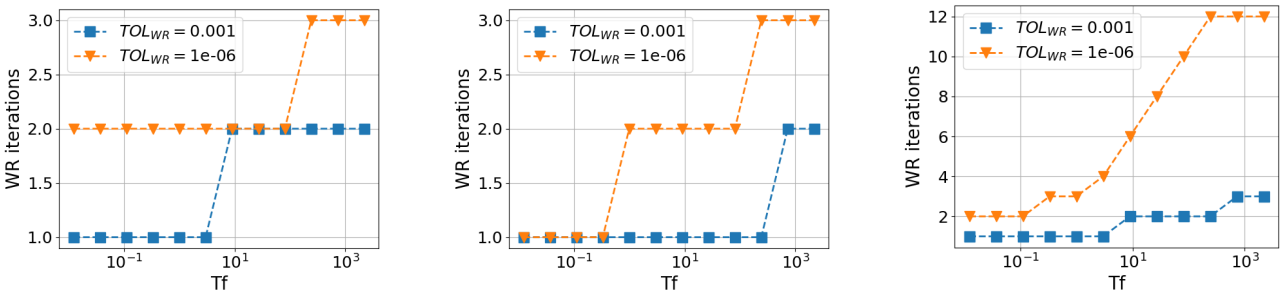

(a) Air-steel (b) Air-water (c) Water-steel

Figure 3: Number of iterations for different time window lengths in the time adaptive case. The x axis is the length of the simulation interval and the y-axis denotes the number of WR iterations it took for it to terminate. Only one time window was used in this test.

Comparing the dependence of the average number of waveform iterations per time window and the number of time windows in Figure 1, one can see that a higher number of time windows yields a reduction in iterations in most cases. This decrease in iterations is largest for $N = 128$, where we see a maximal decrease in the average number of waveform iterations of 33%, 50% and 50% for the air-steel, air-water and water-steel test case respectively. The maximal decrease in iterations is the smallest for $N = 32$ with a decrease of 0%, 33% and 33% for the air-steel, air-water and water-steel test case respectively. The maximal decrease in average waveform iterations for $N = 64$ is between the cases $N = 128$ and $N = 64$.

Furthermore, the average number of waveform iterations have a relation to the cost of the simulation. The cost can be approximated by the number of sub solver calls, since we are solving the underlying systems in the sub-solvers with a direct method. The total number of sub solver calls for our case is given by $k(N_1 + N_2)$, where k denotes the average number of waveform iterations per time window and N_i denotes the total number of timesteps per sub solver for $i = 1, 2$. The only variable that depends on the number of time windows is the average number of waveform iterations k, which decreases with the length of the time window. Thus, using shorter time windows also yields a reduction in the cost of the simulation. For our test case, we achieved a maximal reduction of the cost by a factor of two. Combining this with the fact that the time integration error does not show a strong dependence on the number of time windows yields the recommendation that one should use as short a time window as possible. For equidistant time grids this results in the recommendation to set the number of time windows to the greatest common divisor of N_1 and N_2.

4.2 Time windows and fully time adaptive

In the time adaptive case, a good strategy for the time window length is more difficult to find. The challenge is that the time step size varies with time and is not known beforehand. Thus, to see if one can potentially use the choice of time window to improve the computational efficiency, we first use one time window only and vary the simulation time T_f between 0.012 and 2200. We set Tol_{WR} to 10^{-3} and 10^{-6}.

In Figure 3, we plot the number of wave form iterations against the simulation time T_f. As can be seen, the number of waveform iterations increases slowly with the time window length.

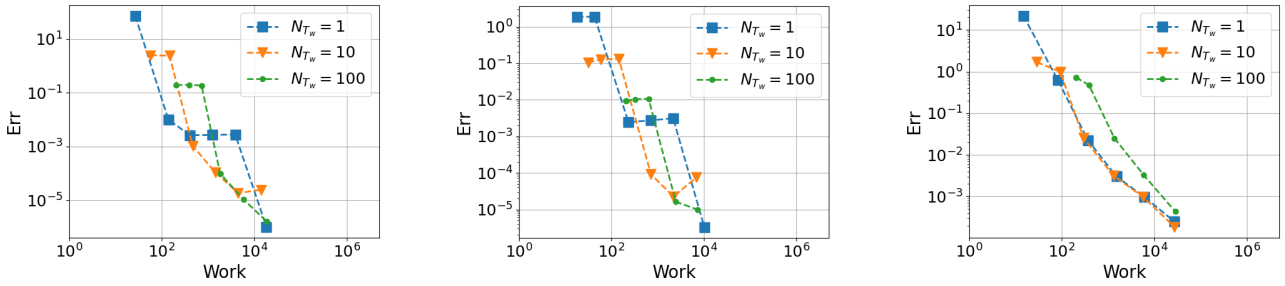

(a) Air-steel (b) Air-water (c) Water-steel

Figure 4: Work over error comparison for different number of equally sized time windows and the tolerance $Tol_{WR} = 10^{-5}$ in the time adaptive case.

This means that one could gain some computational efficiency by selecting a good time window size.

To test how the efficiency of the time adaptive method is affected by the use of time windows, we now use 1, 10 and 100 equally sized time windows for a simulation time of $T_f = 10^4$ and vary Tol_{WR} (and thereby Tol_{TA}). The time integration error was plotted over work in Figure 4. The error is measured using a solution with $Tol_{WR} = 10^{-6}$ and one time window as a baseline. As a measure of work, we again use the number of linear solver calls.

As can be seen in Figure 4, using shorter time windows yields some efficiency increase for a few tolerances. The main problem here is that the time step size varies by many magnitudes between the beginning of the simulation and the end, forcing one either to select fairly big time windows with small increases in performance or using a smaller time window and limiting the time step size to the time window size. Thus, one should use some kind of time adaptive strategy as well for choosing the time window size in the time adaptive case, which is beyond the scope of this paper.

5 Conclusion

Our experiments show that it is beneficial to use as short time windows as possible for the fixed time grid case. For the time adaptive case our results show that using shorter time windows can lead to some gain in computational efficiency in specific cases. However, one would have to use non constant time windows in order to gain a reliable increase in computational efficiency.

REFERENCES

[1] Bellen, A. and Zennaro, M. The use of Runge-Kutta formulae in waveform relaxation methods, *Appl. Num. Math.* (1993) **11(1-3)**:95–114

[2] Janssen, J. and Vandewalle, S. Multigrid Waveform Relaxation on Spatial Finite Element Meshes: The Continuous-Time Case, *SIAM J. Num. Analysis* (1996) **33(2)**:456–474

[3] Janssen, J. and Vandewalle, S. Multigrid Waveform Relaxation on Spatial Finite Element Meshes: The Discrete-Time Case, *SIAM J. Sci. Comput.* (1996) **17(1)**:133–155.

[4] Henshaw, W.D. and Chand, K.K. A composite grid solver for conjugate heat transfer in fluid-structure systems *J. Comput. Phys.* (2009) **228**:2708-3741

[5] Meisriemel, P. *Adaptive time-integration for goal-oriented and coupled problems*. PhD Thesis, Lund University (2021)

[6] Meisrimel, P., Monge, A. and Birken, P. A time adaptive multirate Dirichlet-Neumann waveform relaxation method for heterogeneous coupled heat equations, *ZAMM* (2023), Online first

[7] Monge, A. and Birken P. A Multirate Neumann–Neumann Waveform Relaxation Method for Heterogeneous Coupled Heat Equations *SIAM J. Sci. Comput.* (2019) **41(5)**:86–105.

[8] Monge, A. and Birken, P. On the convergence rate of the Dirichlet–Neumann iteration for unsteady thermal fluid–structure interaction *Comp. Mech.* (2018) **62 (3)**:525-541

[9] Monge, A. *Partitioned methods for time-dependent thermal fluid-structure interaction*. PhD Thesis, Lund University (2018)

[10] Nevanlinna, O. Remarks on Picard Lindelöf iteration I, *BIT Numer. Math.* (1989) **29**:328–346.

[11] Nevanlinna, O. Remarks on Picard Lindelöf iteration II, *BIT Numer. Math.* (1989) **29**:535–562

[12] Gander, M. J., Kwok, F. and Mandal, B. C. Dirichlet-Neumann and Neumann-Neumann waveform relaxation algorithms for parabolic problems, *ETNA* (2016) **45**:424–456

[13] Rüth, B., Uekermann, B., Mehl, M., Birken, P., Monge, A. and Bungartz, H. J. Quasi-Newton waveform iteration for partitioned surface-coupled multiphysics applications, *Int. J. Num. Meth. Engng.* (2021) **122(19)**:5236–5257

[14] Zang, H. A Note on Windowing for the Waveform relaxation method, *Appl. Math. Comp.* (1996) **76(1)**:49-63

[15] Meisrimel, P., Monge, A., Birken, P., https://github.com/PeterMeisrimel/DNWR (last accessed 2023/07/30)